Appendix A
Noise Modeling for AraSim

In this appendix the modeling of thermal noise according to the frequency response of ARA03 is described. This modeling has been performed with information from [1] and under close guidance of Eugene Hong and Dr. Carl Pfendner (both Ohio State University).

The main noise component in ARA is Gaussian distributed thermal noise originating from the ice surrounding the ARA antennas. When Gaussian noise is transformed into the frequency domain by a Fourier transformation, the distribution of the absolute magnitude of events in one frequency bin can be modeled by a Rayleigh distribution:

$$f(x) = \frac{x}{\sigma^2} e^{-\frac{1}{2}\frac{x^2}{\sigma^2}}. \tag{A.1}$$

In Fig. A.1 this distribution is shown for noise events on ARA03. The σ-value of the Rayleigh distribution depends on the frequency response of the recording antenna and signal chain. We can thus use fits of Rayleigh functions to the recorded noise distribution in each frequency bin to model the noise on the ARA stations.

For each frequency bin we generate a random complex number with arbitrary phase and a magnitude following the Rayleigh function obtained by the fit. In the ARA simulation the Box-Muller algorithm is used to generate this complex number [2]. The obtained frequency spectrum is transformed into the time domain by an inverse Fourier transform. The result is a noise waveform which on average follows the fit frequency spectrum of the used data. In this way, a realistic estimation of thermal noise can be obtained. The average spectrum of noise events, simulated with the method described above, compared to the average spectrum of original noise data from station ARA03, is shown in Fig. A.2. In general we find a good agreement. However, for one channel with very low noise amplitude the fits did not converge properly and the response is overestimated in the simulation. This is a small effect and can be neglected in the general result.

T. Meures, *Development of a Sub-glacial Radio Telescope for the Detection of GZK Neutrinos*, Springer Theses, DOI 10.1007/978-3-319-18756-3

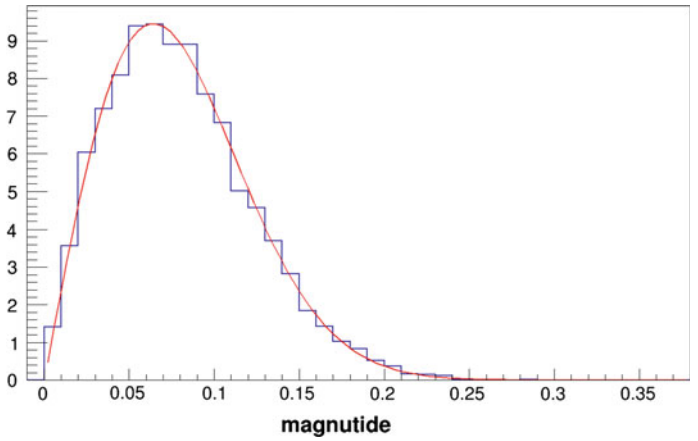

Fig. A.1 The magnitude distribution in mV of a single frequency bin for noise events in ARA03 (*blue*), normalized by the number of data points in the waveform and fit by a Rayleigh function (*red*)

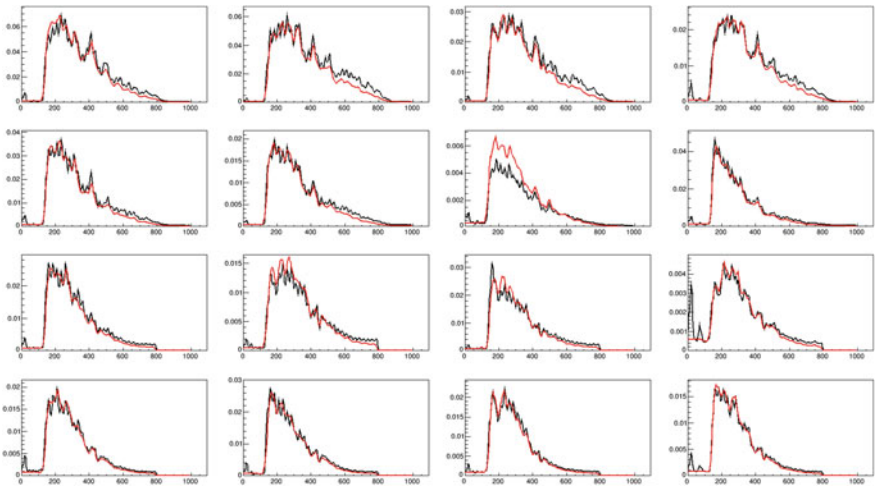

Fig. A.2 The average frequency spectrum for simulated noise events (*red*) and noise events in ARA03 (*black*) for all 16 in-ice antennas. The y-axis shows the magnitude in mV normalized by the number of data points in the waveform, the x-axis shows the frequency in MHz

Appendix B
Details on the Systematic Error Estimation

In Sect. 10.2 we summarized the derivation of systematic errors on the analysis presented in this thesis. In the following we explain a few more details on the energy dependence and on selected error estimations.

Fig. B.1 shows the relative systematic errors on the effective area as function of energy at trigger level (a) and after application of the analysis cuts (b). One finds that uncertainties on the attenuation length and the analysis efficiency only have a mild influence on the effective area and do not show a strong energy dependence. The biggest contributions to the error originate from the uncertainties on the cross section and on the signal chain. Their dominance shifts with energy: at low energies the error on the signal chain is the strongest while at higher energies the cross section error becomes dominant. In the following, the origin of these influences is described in more details.

The strong influence of the signal chain at low energies is due to the fact that the signal amplitudes of most events are close to the trigger threshold. At higher energies the signal abundantly exceeds the threshold and a degradation or elevation does not have a strong influence on the trigger and analysis efficiency.

The error on the cross section arises from the fact that the neutrino interaction cross section at the energies of GZK neutrinos is unmeasured but has to be extrapolated using theoretical calculations. Uncertainties go up to 100 % at 10^{20} eV [3]. This error affects mostly the neutrinos reaching the detector through the Earth. Their contribution to the effective volume is however very small (Fig. B.2a) and consequently a mild influence of the cross section on the effective volume is observed (Fig. B.2b). For this reason, the error on the effective area is proportional to the uncertainty of the cross section (see Eqs. 7.2 and 7.3) and grows with rising energy.

The error on the analysis efficiency is calculated using the SNR comparison between simulated data and calibration pulsers, as shown in Figs. 8.7, 8.8, 8.21 and 8.23. The same distributions are produced for each energy bin separately and analysis cuts are applied. For SNR bins of $width = 1$ the cut efficiency on calibration pulser events and simulated events is compared and the difference is used as the systematic error for that bin. The analysis efficiency for simulated neutrinos with a primary energy of 10^{18} eV compared to calibration pulser events on ARA03 is shown in

T. Meures, *Development of a Sub-glacial Radio Telescope for the Detection of GZK Neutrinos*, Springer Theses, DOI 10.1007/978-3-319-18756-3

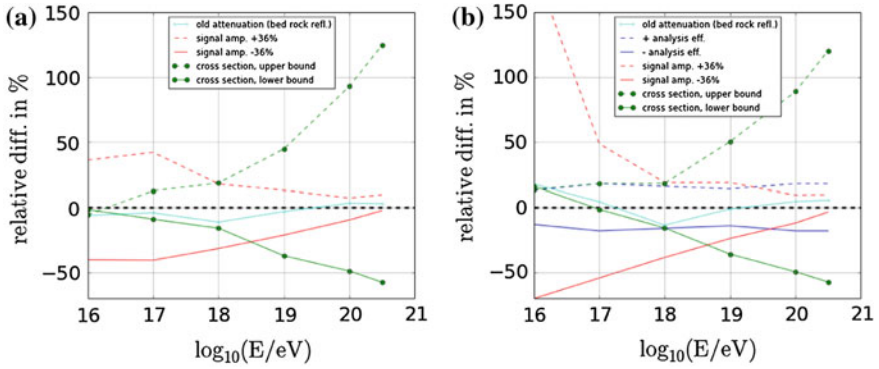

Fig. B.1 The relative changes due to systematic uncertainties on given input parameters plotted versus energy: **a** at trigger level, **b** after analysis cuts

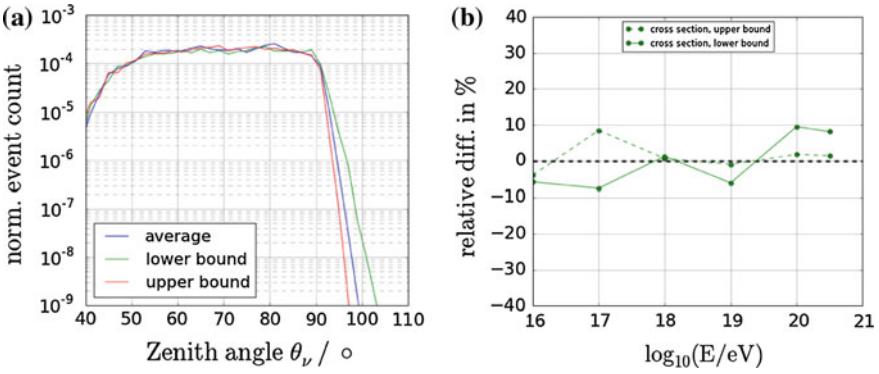

Fig. B.2 **a** The acceptance of the two ARA stations versus zenith angle of the incoming neutrino at 10^{19} eV at differently assumed interaction cross sections, according to the values and uncertainty bounds derived in [3]. **b** The relative difference of the effective volume of the two ARA stations for cross sections assumed at the *upper* and *lower* uncertainty bound, compared to the average value

Fig. B.3. The bias on the SNR value for pure noise has been calculated to 1.9 ± 0.2. Therefore, only events with $SNR > 2$ are used for the error estimation. The final error for a given neutrino energy is derived as the mean value of the differences in efficiency $\Delta_{eff,i}$, weighted by the number of triggering events N_i in a SNR bin i:

$$\sigma_{sys} = \frac{\sum \left(|\Delta_{eff,i}| \cdot N_i \right)}{\sum N_i}. \tag{B.1}$$

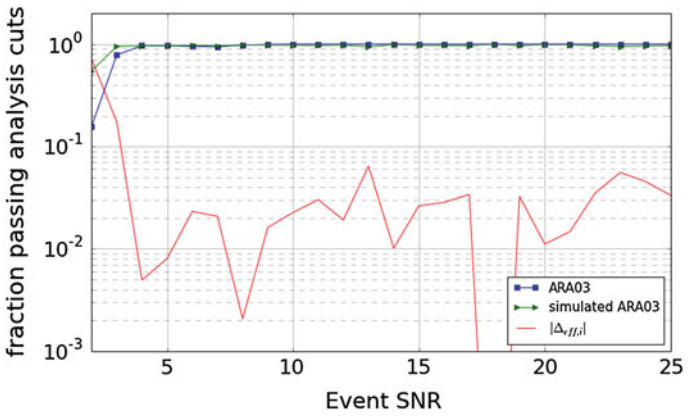

Fig. B.3 The analysis efficiency for simulated neutrino events (*green*) with a primary energy of 10^{18} eV and calibration pulser events on ARA03 (*blue*). The difference in efficiency is plotted in *red*

One should note that most of the simulated events have a low SNR which is why these bins get the strongest weight. To give one example the derived relative systematic error for 10^{18} eV is 16 %.

References

1. M.J. Mottram, A Search for Ultra-high Energy Neutrinos and Cosmic-Rays with ANITA-2. PhD dissertation, University College London, 2012
2. G.E.P. Box, M.E. Muller, A note on the generation of random normal deviates. Ann. Math. Stat. **29**(2), 610–611 (1958)
3. A. Connolly, R.S. Thorne, D. Waters, Calculation of high energy neutrino-nucleon cross sections and uncertainties using the Martin-Stirling-Thorne-Watt parton distribution functions and implications for future experiments. Phys. Rev. D **83**, 113009 (2011)